# DEVELOPMENT OF THE MICROSTRUCTURE AND TEXTURE OF A STRIP CAST AUSTENITIC STAINLESS STEEL DURING COLD ROLLING AND ANNEALING

**MAX-PLANCK PROJECT REPORT**

***Dierk Raabe***

***Max-Planck-Institut für Eisenforschung***
***Max-Planck-Str. 1***
***40237 Düsseldorf***
***Germany***

*April, Max-Planck-Society*
*http://www.mpg.de http://www.mpie.de http://edoc.mpg.de/*

# Project References

D. Raabe, M. Hölscher, F. Reher, K. Lücke: Scripta Metall. 29 (1993) 113–116
„Textures of strip cast Fe-16% Cr“

M. Hölscher, D. Raabe, K. Lücke: Steel Research 62 (1991) 567–575
„Rolling and recrystallization textures of bcc steels“

D. Raabe, Steel Research 74 (2003) 327-337
“Overview on basic types of hot rolling textures of steels”

D. Raabe, M. Hölscher, M. Dubke, H. Pfeifer, H. Hanke, K. Lücke: Steel Research 4 (1993) 359–363
„Texture development of strip cast ferritic stainless steels“

D. Raabe, K. Lücke: Materials Science and Technology 9 (1993) 302–312
„Textures of ferritic stainless steels“

D. Raabe: Metallurgical and Materials Transactions A 26A April (1995) 991–998
„Microstructure and crystallographic texture of strip cast and hot rolled austenitic stainless steel“

D. Raabe: Materials Science and Technology 11 (1995) 461–468
„Textures of strip cast and hot rolled ferritic and austenitic stainless steel“

D. Raabe: Acta Materialia 45 (1997) 1137–1151
„Texture and microstructure evolution during cold rolling of a strip cast and of a hot rolled austenitic stainless steel“

**Keywords:** Austenitic Stainless Steel, Strip Casting, Transformation Selection, Card Glide, Simulation, Texture

## ABSTRACT

The microstructure and texture of a strip cast, cold rolled and annealed austenitic steel with 18% Cr and 8.5% Ni (%=mass%) was studied. The microstructure of the cast strip showed globular grains with martensite in the center layer and blocks of austenitic dendrites in the other layers. The cast sample had a weak {001}<uvw> texture which was attributed to growth selection. During rolling the volume fraction of martensite increased up to ~50 vol.% (ε=80%). The rolling texture of the austenite was characterized by {011}<211> and {011}<100>. It was simulated by means of a Taylor model considering grain interaction and the card glide mechanism. The texture was only weakly changed during annealing.

## INTRODUCTION

Stainless steel sheets are manufactured by continuous casting, hot rolling, cold rolling and annealing. However, recent progress in producing steel sheets in pilot-scale unequal-diameter twin roll strip casters (Fig. 1) has stimu-lated efforts to convert such devices to commercial pro-duction [1-3]. Strip casting provides some improvements compared to conventional methods. First, it supplies a band with the same geometry as produced by hot rolling [1-3]. This permits to bypass hot rolling. Second, the weak texture of the cast strip reduces anisotropy [4,5]. Third, the high solidification rate leads to refined microstructures when compared to ordinary casting. Fourth, it is possible to directly cast steel sheets which are not endowed with a sufficient intrinsic ductility for rolling, such as transformer steels with a high Si content [6]. Fifth, it is not economical to produce small quantities of high grade steels by continuous casting and hot rolling.

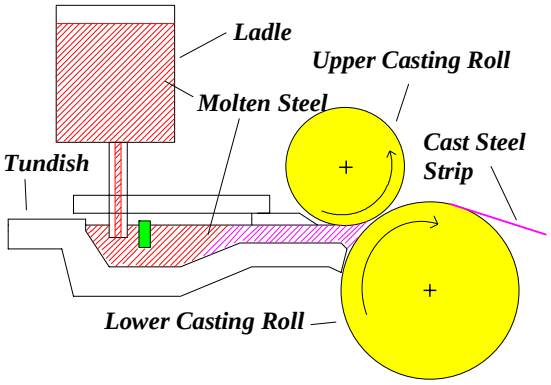


Fig. 1 Unequal-diameter twin roll strip caster.

## EXPERIMENTAL

The sample contained 0.05% C, 0.76% Si, 1.37% Mn, 18.1% Cr, 0.24% Mo, and 8.54% Ni (%=mass%). The strip cast specimen was produced on a pilot-scale unequal-diameter twin roll caster [1,2]. In this machine liquid steel was cast into a preheated tundish which contacted two rotating water cooled steel rolls. The steel solidified as a thin film on the roll surfaces just before reaching the bite of the rolls. The process was conducted in such a way, that the contact length between the liquid metal and the roll surface was equal for both rolls. In the roll gap the films impinged and were hot compressed, receiving a thickness reduction of about 15%. The strip left the gap with a temperature of about 1370 K and a thickness of 2.4 mm. Prior to cold rolling the sample was annealed (1370 K, 20 minutes) and descaled. Cold rolling was carried out to $\varepsilon$=80% ($\varepsilon$ : thickness reduction $\Delta d/d_0$).

The textures were examined by measuring the pole figures {111}, {200}, {220} and {113} of the austenitic phase and {110}, {200}, {211} and {103} of the martensitic phase using $Mo_{K\alpha}$ radiation. However, the {111} Bragg angle of the austenite overlapped the {110} Bragg angle of the martensite. For avoiding ambiguities thus both the {110} pole figures of the martensite and the {111} pole figures of the austenite were ignored for computing the respective orientation distribution functions (ODF) ($l_{max}$=22) [7,8]. The results obtained by using non overlapping pole figures were confirmed by using corrected overlapping pole figures. For this purpose the ODFs of the martensite the volume fraction of which increased from 22 vol.% ($\varepsilon$=20%) up to 52 vol.% ($\varepsilon$=80%) during rolling were computed using the non overlapping {200}, {211} and {103} pole figures. Subsequently, the {110} projection was recalculated and subtracted from the experimental $\{111\}_{fcc}$ + $\{110\}_{bcc}$ pole figure. The subtraction was weighted by the metallographically determined volume fraction of the martensite. After correction and normalization the ODFs of the austenitic phase were finally recalculated [7,8]. Indeed, the results were identical to the ODFs computed from the three non-overlapping pole figures. However, this analysis gave an idea of possible errors (up to 18% in case of Goss) in former texture studies on austenitic steels which used overlapping pole figures.

Relevant fibers for austenite textures are the $\alpha_{fcc}$-fiber (<011> parallel to the normal direction (ND)), the $\beta$-fiber (less symmetric fiber comprising {211}<111>, ~{123}<634> and {011}<211>), and the cube fibers showing rotations of {001}<100> about rolling (RD), transverse (TD) and ND. Frequent texture components are indicated by names, such as the ‘Brass’ or ‘B’, {011}<211>, the ‘Copper’ or ‘C’ {211}<111>, the ‘S’ ~{123}<634>, the ‘Goss’ {011}<100>, and the ‘Cube’ component, {001}<100>.

## RESULTS AND DISCUSSION

Between the surface and the near-center layers (0.4≤s≤1.0) the microstructure of the strip cast austenite showed uniformly oriented blocks of primary dendrites. The parameter s indicates the ratio between the distance of the actual layer from the center layer and the half thickness. The blocks had an average diameter of 140 μm and a length of up to 500 μm parallel to their respective growth direction. The microsegregated interdendritic regions appeared dark whilst the austenite appeared bright. Siegel et al. [9] showed that both Ni and Cr are enrich whilst Fe is depleted between the dendrites. Close to the center layers (0.1≤s≤0.3) a more blocky and nearly equiaxed austenite morphology with some martensite was observed. In the center layer (0.0≤s≤0.1) a globular austenitic grain structure with martensite platelets appeared. During cold rolling the blocks flattened and revealed partial strain induced phase transfor-mation from austenite to martensite.

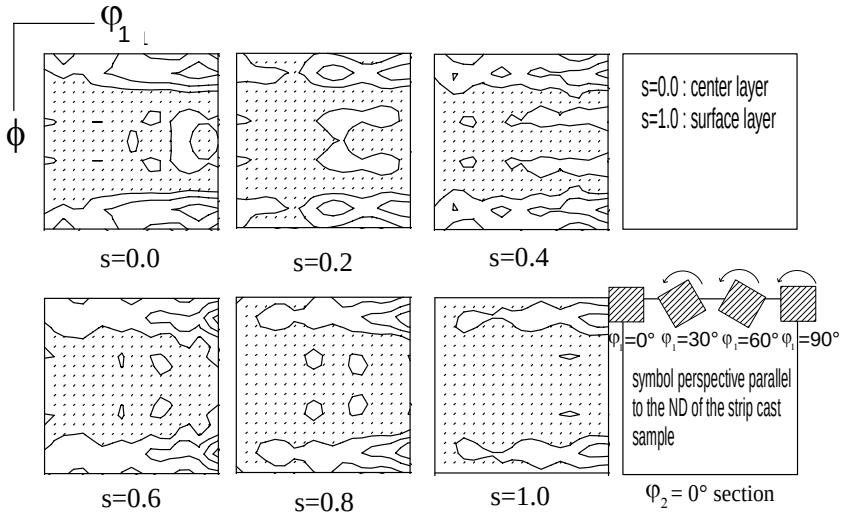


Fig. 2 Experimental texture of the strip cast austenitic steel.

The texture of the strip cast material showed in all layers a weak {001}<uvw> texture fiber (Fig. 2) which was attributed to growth selection. From directional solidification experiments on Al it is known that {100}<uvw> has a larger growth rate than other orientations [10]. The cold rolling texture was characterized by the fibers β and $\alpha_{fcc}$ (Fig. 3), the former one being dominated by the B component which indicates a resemblance to brass and stable austenite [11,12]. However, the latter fiber shows that at large strains the texture deviates from that of single phase brass (70/40, 63/37) and two phase brass (60/40, 20 vol.% bcc phase) [13,14]. For 50<ε<70% the B orientation is no longer the dominant component but accompanied by a Goss orientation of similar orientation density. After strong thickness reduction (ε=80%) the orientation density of the Goss even exceeds that of the B component.

For explaining the strong B component the approach of Kocks and Necker [15] is adopted which suggests a re-interpretation of the card glide process. This mechanism which was originally proposed by Hu [16], is based on a fixed {111} glide plane in which slip can operate with arbitrary Burgers vectors. Both the activation of <110> and partial <211> glide vectors is conceivable. However, plastic flow through single <211> Shockley type slip vectors is not likely since it would imply excessive faulting. For this reason, Kocks and Necker [15] pointed out that net <211> slip can as well be achieved by simultaneous glide employing two conventional <110> translation vectors which similarly contribute to shear and add up to a net <211> vector. Such a situation is possible at least in the vicinity of polyslip vertices of the yield surface. For checking this approach the rolling textures were simulated using a modified Taylor model which considers grain interaction [17] and the card glide mechanism, where the net <211> slip vectors are not interpreted as partial slip vectors but as simultaneously contributing <110> vectors. In the simulation the ratio between the critical resolved shear stress (CRSS) for slip in the net <211> and <110> directions, $\alpha = \tau_{<211>}/\tau_{<111>}$, was varied between $2/\sqrt{3}$ and 0.96 [15]. In all simulations an ideal plane strain state was prescribed. The textures were computed up to $\varepsilon$=80%, starting from a random texture consisting of 936 orientations. The ODFs were calculated using Gauss functions with a scatter width of 11°. For $\alpha$ values between $2/\sqrt{3}$ and 0.98 a weak agreement with experiment was observed. However, for $\alpha$=0.96 the prediction was in better accord with experiment except for one main deviation, namely the strong occurrence of Goss (Figs. 3, 4). Later, it will be shown that the dominance of Goss can be explained in terms of the transformation behavior, rather than in terms of card glide. Provided that the card glide mechanism has a physical basis at least for orientations in the vicinity of polyslip vertices of the yield surface, it is concluded that the corresponding (pseudo) CRSS ratio has a value slightly below 1.

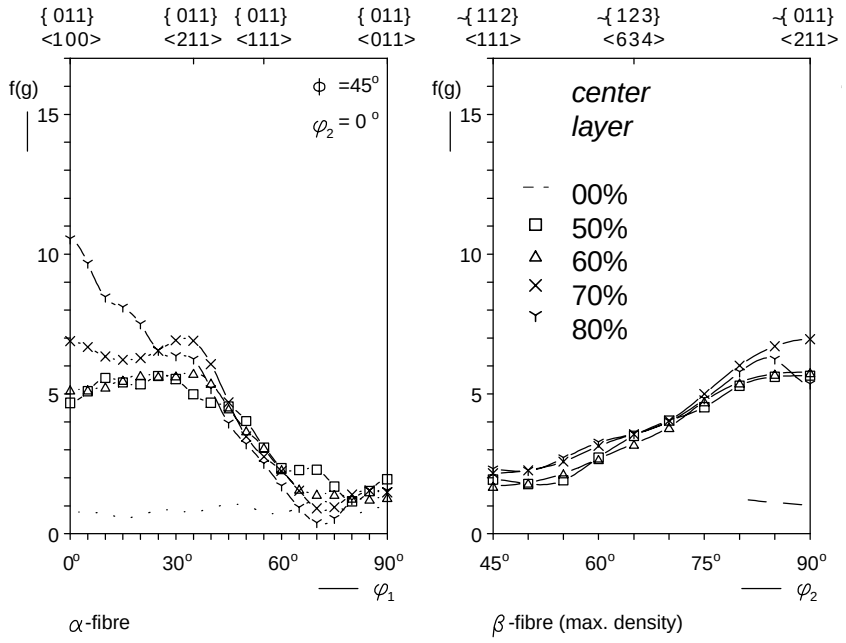


Fig. 3 Experimental texture of the strip cast austenitic steel.

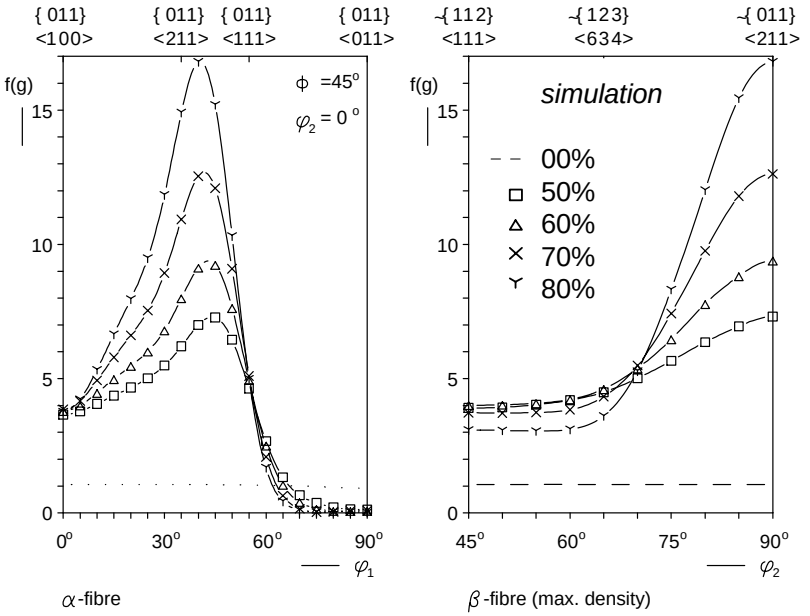


Fig. 4 Taylor simulation, card glide, α=0.96.

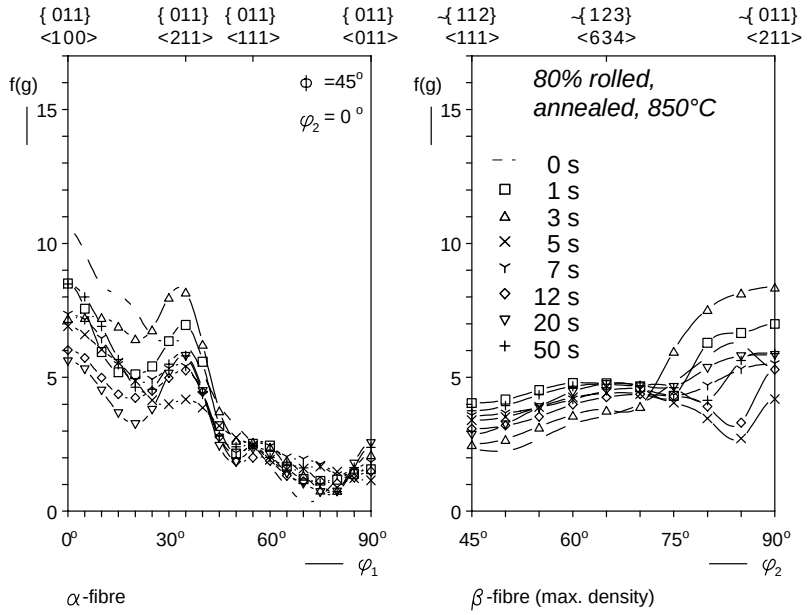


Fig. 5 Annealing, 80% cold rolled, annealed at 850°C.

It is worth to emphasize that both the experimental and simulated (α=0.96) data are very similar to 90° about the TD rotated textures of bcc materials. In a former study [18] which focused on the similarity of fcc and bcc rolling textures it was shown that an identity of both texture types indeed results under particular strain constraints. Further deviations which became apparent especially on the respective α-fibers were attributed to the fact that in bcc two or even three rather than only one type of slip system are typically active. This argument does obviously no longer hold for fcc alloys which deform via {111}<110> and net {111}<211> glide systems since they correspond to the 90° about the TD rotated bcc {110}<111> and {112}<111> glide systems. As mentioned earlier [15] the card glide mechanism in fcc thus corresponds to the 90° about the TD rotated pencil glide mechanism in bcc.

The second main observation, i.e. the dominance of Goss already at intermediate strains (Fig. 3) is not typical of fcc metals with a low SFE, e.g. brass. However, besides the various similarities such as SFE there is one main difference between the present stainless steel and comparable dual phase brasses [13,14], namely the fact that in the present alloy a strain induced and strictly crystallographic phase transformation from austenite to martensite occurs during cold rolling.

Goodchild et al. [19] investigated the martensitic phase transformation at various temperatures in two austenitic stainless steels with 17.36% Cr, 7.2% Ni and 17.36% Cr, 7.2% Ni, respectively (%=mass%). They observed that after tensile deformation in the unstable temperature region martensite was formed in all grains except in those extended along <001>. Conversely, compressive deformation caused transformation in grains compressed along <001> but not in grains in which the compression axis was close to <011>. This observation is of substantial relevance to the interpretation of the present textures. Prescribing a Tucker type stress state [20] any orientation which has a <011> direction parallel to the compression axis (ND) and a <100> direction parallel to the tensile axis (RD) will be stable with respect to strain induced phase transformation. This criterion is fulfilled for {011}<100> (Goss). The B orientation, {011}<211>, reveals likewise a <011> direction parallel to the ND, but no <100> direction parallel to the RD. It is thus conceivable that the B orientation is less stable with respect to martensitic phase transformation than the Goss component. In analogy to variant selection, where particular martensite variants prevail due to external or internal constraints, the present phenomenon will hereafter be referred to as transformation selection.

If the B component would indeed undergo selective martensitic phase transforma-tion during cold rolling one would expect two characteristic texture changes. First, the preferred transformation of B should lead to a degradation or at least a stagnation of its orientation density in the fcc texture. Second, its selective transformation should entail a new texture component in the martensite characterized by a strict crystallographic relation-ship to the B component. The first conclusion is indeed co-vered by the textures shown in Fig. 5. The second prediction was found as well and will be discussed in a subsequent report [21].

Fig 5 shows the annealing textures (T=850°C, salt bath) of the 60% rolled sample. Although the defor-mation microstructure is gradually removed during the anneal the texture shows only weak chan-ges compared to the rolling textures. The microstructure substantiates that the segregated deformation microstructure (striped areas) is homogenized during annealing (bright areas). This beneficial effect could be due to the diffusion coefficient which is larger in the moving large grain boundary than in the bulk, provided that primary recrystallization is the leading mechanism. The weak change of the cold rolling texture during annealing was also observed in previous investigations [11,12]. However, the discussion of the present annealing textures is complicated by the fact that the initial microstructure of the cast material was less homogeneous than that of a conventional hot band sample. Thus, some additional effects must be con-sidered, such as the influence of segregation and of the deformation martensite which becomes instable upon annealing. Details of the recrystallization textures will be discussed in a subsequent report [21].

## SUMMARY AND CONCLUSIONS

The development of the microstructure and crystallographic texture of a strip cast austenitic stainless steel (18 mass% Cr, 8.5 mass% Ni) during cold rolling and annealing has been studied. The main observations and conclusions are :

The strip cast sample revealed a weak texture fiber close to {100}<uvw>, which was attributed to growth selection.

During cold rolling the sample revealed a strong B and an even stronger Goss component (ε=80%). This phenomenon was explained in terms of transformation selection. Based on the results of Goodchild et al. [19] it was suggested that the Goss component remained stable whilst the B orientation was unstable with respect to strain induced martensitic transformation.

The cold rolling texture, especially the pronunciation of the B orientation, was simulated by using the card glide mechanisms suggested by Hu [16] but in the re-interpretation of Kocks and Necker [15]. The best agreement between experiment and prediction was achieved for simulations in which the ratio between the critical resolved shear stress (CRSS) for slip in the <211> and <110> directions was equal to 0.96. The strong Goss component was not covered by the model. This deviation was attributed to the influence of the martensite.

The annealing textures did only weakly deviate from the cold rolling textures.

## REPORT REFERENCES

1. R. Hentrich, M. Dubke, H.J. Funk, K. Hanke, J. Loh & S. Kuhlmann: Stahl u. Eisen 111 (1991), 51.
2. D. Raabe, M. Hölscher, M. Dubke, H. Pfeifer, K. Hanke & K. Lücke, Steel Research 64 (1993), 359.
3. B. Q. Li, Journal of Materials (JOM) 47 (1995), 13.
4. D. Raabe, Metallurgical and Materials Transactions A 26A (1995), 991.
5. D. Raabe, Materials Science and Technology, 11 (1995), 461.
6. K. Shibuya and M. Ozawa, ISIJ International 31 (1991), 661.
7. H. J. Bunge and C. J. Esling, Physique- Lettr. 40 (1979), 627.
8. M. Dahms, Textures and Microstructures 19 (1992), 169.
9. U. Siegel, H.-J. Spies and H.-J. Eckstein, Steel Research 57 (1986), 25.
10. J. Hirsch, E. Nes and K. Lücke, Acta metall. 35 (1987), 427.
11. C. Donadille, R. Valle, P. Dervin and R. Penelle, Acta metall. 37 (1989), 1547.
12. T. J. Rickert , Materials Science Forum, 157-162 (1994), 2017.
13. K. Mäder, E. Hornbogen, Scripta metall. 8 (1974), 979.
14. O. Engler, J. Hirsch and K. Lücke, Zeitschrift Metallkunde 86 (1995), 465.
15. U. F. Kocks and C. T. Necker, Proc. 15th RISØ Int. Symp. on Mat. Sc. 'Num. Pred. of Deform., Processes and the Behaviour of Real Materials', edited by S. I. Andersen, J. B. Bilde-Sorensen, T. Lorentzen, O. B. Pedersen and N. J. Sorensen, RISØ National Lab., Denmark (1994), 45.
16. H. Hu, R. S. Cline and S. R. Goodman, in Proc. of ASM Seminar on 'Recrystallization, Grain Growth and Textures', edited by H. Margolin, American Society of Metals, Metals Park, Ohio, 295 (1966).

17. U. Schmitter, Diploma Thesis, University of Technoligy (RWTH) Aachen, Institut für Metallkunde und Metallphysik, K. Lücke (1993).
18. M. Hölscher, D. Raabe, K. Lücke, Acta metall. 42 (1994), 879.
19. D. Goodchild, W. T. Roberts and D. V. Wilson, Acta metall. 18 (1970), 1137.
20. G. E. G. Tucker, Acta metall. 12 (1964), 1093.
21. D. Raabe, in press.